ARCHIVES
of Pathology & Laboratory Medicine
Reprinted from Vol.139(6)

Determination of Genotypes Using a Fully Automated Molecular Detection System

Gwendolyn Spizz, PhD; Zongyuan Chen, PhD; Peng Li, PhD; I. Cristina McGuire, PhD; Paulina Klimkiewicz, BS; Devin Zysling, PhD; Rubina Yasmin, PhD; Whitney Hungerford, BS; Benjamin Thomas, BS; Gregory Wilding, PhD; Gregory Mouchka, MS; Lincoln Young, BS; Peng Zhou, PhD; Richard A. Montagna, PhD

• ***Context.***—**Although the value of pharmacogenomics to improve patient outcomes has become increasingly clear, adoption in medical practice has been slow, which can be attributed to several factors, including complicated and expensive testing procedures and required equipment, lack of training by private practice physicians, and reluctance of both private and commercial payers to reimburse for such testing.**

Objectives.—**To evaluate a fully automated molecular detection system for human genotyping assays, starting with anticoagulated whole blood samples, and to perform all sample preparation, assay, and analysis steps automatically with actionable results reported by the system's software.**

Design.—**The genotypes of 254 random individuals were determined by performing bidirectional DNA sequencing, and that information was used to statistically train the imaging software of the automated molecular detection system to distinguish the 3 possible genotypes (ie, homozygous wild type, heterozygous, and homozygous mutant) at each of 3 different loci (*CYP2C9*2, CYP2C9*3,* and *VKORC1*).**

Results.—**The resulting software algorithm was able to correctly identify the genotypes of all 254 individuals (100%) evaluated without any further user analysis.**

Conclusions.—**The EncompassMDx workstation (Rheonix, Inc, Ithaca, New York) is a molecular detection system that can automatically determine the genotypes of individuals in an unattended manner. Considerably less technical expertise was required to achieve results identical to those obtained using more complex, time-consuming, and expensive bidirectional DNA sequencing. This optimized system may dramatically simplify and reduce the costs of pharmacogenomics testing, thus leading to more-widespread use.**

(*Arch Pathol Lab Med.* 2015;139:805–811; doi: 10.5858/arpa.2014-0059-OA)

Pharmacogenomics data are now available to provide "personalized" or "precision" medicine (PM) information that can help to precisely tailor treatments by delivering specific drugs at optimized doses to specific patients.[1] Despite the promise of PM, however, adoption in medical practice has been slow.[2] Test complexity and cost, along with a lack of training and understanding of pharmacogenomics by many private practice physicians, is partly to blame. Reluctance by private and commercial payers to reimburse pharmacogenomics tests also has a significant role.[3] Payers base reimbursement decisions on many factors, including clinical utility, cost-effectiveness, demand by physicians and patients, and recommendations and guidelines from professional societies. Ironically, although effective use of PM could help drive down costs, health care costs continue to escalate on a worldwide basis. In the United States, total expenditures on health care have risen from approximately 9.5% of gross domestic product in 1980 to approximately 17.5% in 2009,[4] with other countries experiencing similar increases. Although many factors contribute to these increases, effective use of PM has the potential to improve clinical outcomes and thereby help to lower health care costs. To gain more widespread use and acceptance of PM, it would be helpful to reduce the costs and complexity of pharmacogenomics testing.

An example of the dichotomy between available pharmacogenomics data and use concerns the anticoagulant warfarin, which is the most frequently prescribed anticoagulant on a worldwide basis. Its extensive use and narrow therapeutic index contributes to among the highest worldwide, adverse drug events (ADEs).[5–8] Current standards of care[9] incorporate initial empiric dosing of warfarin based on various clinical factors with adjustment to the dose based on periodic prothrombin time and international normalized ratio (INR) testing to achieve a stable INR of 2 to 3. The

Accepted for publication August 8, 2014.

Supplemental digital content is available for this article at www.archivesofpathology.org in the June 2015 table of contents.

From Rheonix, Inc, Ithaca, New York (Drs Spizz, Chen, Li, McGuire, Zysling, Yasmin, Zhou, and Montagna; Mss Klimkiewicz and Hungerford; and Messrs Thomas, Mouchka, and Young); and the Department of Biostatistics, State University of New York, Buffalo (Dr Wilding). Dr Li is now with Thermo Fisher Scientific, San Francisco, California; Ms Klimkiewicz is now with the Rochester Institute of Technology, Rochester, New York; and Mr Young is now with INEng, LLC, Ithaca, New York.

With the exception of Dr Wilding, who is a Rheonix paid consultant for biostatistical matters, all authors were employees of Rheonix during the study, and some authors own stock in Rheonix (Drs Spizz, Chen, Li, McGuire, Zhou, and Montagna, and Messrs Mouchka and Young).

Reprints: Richard A. Montagna, PhD, Rheonix, Inc, 10 Brown Rd, Ithaca, NY 14850 (e-mail: Rmontagna@rheonix.com).

Table 1. Alignment of Flanking Regions Evaluated for Each Single Nucleotide Polymorphism (SNP) Analyzed[a]

Target	Upstream	SNP	Downstream
*CYP2C9*2* forward	CATTGAGGAC	[T/C]	GTGTTCAAGA
*CYP2C9*2* reverse	TCTTGAACAC	[G/A]	GTCCTCAATG
*CYP2C9*3* forward	CCAGAGATAC	[A/C]	TTGACCTTCT
*CYP2C9*3* reverse	AGAAGGTCAA	[T/G]	GTATCTCTGG
VKORC1 forward	GATCATCGAC	[T/C]	CTTGGACTAG
VKORC1 reverse	CTAGTCCAAG	[A/G]	GTCGATGATC

[a] Alignment of 10 nucleotides upstream and downstream of each of the 3 targeted SNPs (shown 5′ to 3′).

potential for an ADE is greatest during the initial phase of therapy, where subtherapeutic doses can increase the risk for thromboembolic events and supratherapeutic doses can increase the risk for major bleeding events. Several pharmacogenomics algorithms have been developed[10–12] to reduce those risks, based on single nucleotide polymorphisms (SNPs) in the cytochrome P450, family 2, subfamily C, polypeptide 9 (*CYP2C9*) and vitamin K epoxide reductase complex, subunit 1 (*VKORC1*) genes.[13] The *CYP2C9*2* and *CYP2C9*3* variants are associated with a decrease in the breakdown of active warfarin; thus, a lower dose of the drug is required to achieve a therapeutic INR. Mutations in *VKORC1*, which is responsible for activation of vitamin K–dependent clotting factors, decrease the conversion of vitamin K–epoxide to vitamin K; therefore, lower doses are required in individuals carrying the mutant allele.[14] Because of this information, current US Food and Drug Administration (FDA)–approved drug labeling for warfarin includes 3 ranges of expected maintenance doses (Supplemental Table 1) (see supplemental material file at www.archivesofpathology.org in the June 2015 table of contents) based on a patient's *CYP2C9* and *VKORC1* genotypes.[15] In addition, the FDA has required similar pharmacogenomics information on the labeling of other prescription drugs.[1]

Despite the potential for genetic data to reduce ADEs associated with warfarin dosing, many insurers do not reimburse the costs of the necessary pharmacogenomics testing. Limited studies demonstrating clinical utility and the high cost of genotype testing, as compared with prothrombin time and INR testing, are often cited as reasons for reduced use and reimbursement.[16]

Toward reducing the complexity and costs associated with pharmacogenomics testing, the goal of this study was to demonstrate that an existing microfluidic platform[17] could be used in pharmacogenomics testing. Without any user intervention, the system automatically performs all sample preparations, multiplex polymerase chain reaction (PCR) analyses, and readout steps. Although the present work focused on pharmacogenomics applications, similar development efforts are currently underway to expand the use of the system to infectious disease, oncology, and hospital-acquired infection applications, as well as nonclinical markets, such as food, beverage, and animal health testing.

To fully automate the readout of genotypes, the current efforts focused on optimizing the computational software to work in conjunction with the system's optics to evaluate the intensity of the hybridization spots on the DNA array and to report the genotypes at multiple loci. Using analysis of the *CYP2C9*2*, *CYP2C9*3*, and *VKORC1* loci as a model system, individual blood samples from 320 deidentified individuals were subjected to bidirectional DNA sequencing,[18] and the sequencing results were used to train the imaging software to distinguish the 3 different genotypes (ie, homozygous wild type, heterozygous, and homozygous mutant) at each of the 3 loci.

METHODS

Bidirectional DNA Sequencing

Tubes of EDTA anticoagulated blood samples (300 μL aliquots) were sent to the State University of New York (Buffalo) Center for Advanced Biomedical and Bioengineering Technology for DNA purification and bidirectional sequencing following standard operating protocols. Briefly, the QIAamp DNA Blood BioRobot kit (Qiagen, Valencia, California) was used for DNA purification followed by PicoGreen (Life Technologies, Carlsbad, California) double-stranded DNA quantitation. Target regions of interest were amplified (PCR primer sequences shown in Supplemental Table 2), and the amplicons were purified with the QIAquick PCR Purification Kit (Qiagen) and quantitated with PicoGreen using the Applied Biosystems 3730 DNA Analyzer (Life Technologies). Sequences were evaluated by 2 independent analysts (R.M. and S.G.) and 2 different software programs (SeqMan, DNASTAR, Madison, Wisconsin; and CLC Main workbench, CLC bio, Boston, Massachusetts). Twenty nucleotide regions flanking the individual SNPs (Table 1) were aligned for all sequences and evaluated for the allele. Any discrepancies observed between the 2 analysts were reviewed by a third analyst (G.S.) and, if necessary, resequenced.

Analysis of Deidentified Individual Blood Samples

A EncompassMDx workstation and disposable CARD cartridges (Rheonix, Inc, Ithaca, New York) (hereinafter, *CARD*) were used to process each sample. Briefly, the assays were initiated with the manual addition of 15 μL of EDTA anticoagulated, whole blood samples or the addition of controls into the sample or application port of the CARD (Supplemental Figure 1); each CARD is capable of simultaneously analyzing 4 separate samples. All other reagent additions were automatically performed by the software-driven robotics of the system, which is capable of automatically processing 16 samples per run. Within the sample preparation portion of the CARD (Supplemental Figure 1, zone 1), the cells were lysed, and nucleic acids were extracted and purified by a modified Boom et al[19] method optimized for compatibility with the plastics and pump-driven microfluidics of the CARD. The DNA eluted from the silica filter column was then metered into 2 separate fluidic channels and allowed to flow into separate PCR reaction chambers (Supplemental Figure 1, zone 2), where PCR amplification was performed using primer pairs biotinylated at their 5′ termini. The PCR primer pairs and buffer conditions, optimized to amplify the *CYP2C9*2* and *CYP2C9*3* loci, were used in a single multiplex assay in one PCR reaction chamber, whereas the second chamber contained the primer pairs and buffer conditions, optimized to amplify the *VKORC1* loci. Amplification took place within the onboard thermocycler, with both PCR chambers being subjected to the same thermocycling conditions. After completion of the PCR, hybridization buffer was pumped into the PCR reaction chambers, diluting the biotinylated, amplified products, which was followed by heat denaturation of the diluted mixes. Finally, both mixes were pumped to the DNA array portion of the CARD (Supplemental Figure 1, zone 3). Following hybridization of the single-stranded, biotinylated DNA, strands captured by immobilized DNA probes were detected via incubation with horseradish peroxidase (HRP)–conjugated streptavidin followed by the 3,3′,5,5′-tetramethylbenzidine (TMB) substrate.

The unique pumps and valves[17] resulting from the manufacturing process[20] drive the fluidic movements to accomplish all steps, from lysis through color development, while keeping the fluids compartmentally sealed from the external environment and preventing any possibility of contamination. Spot color intensity from the precipitated product of the HRP-TMB reaction is captured by the optics system of the EncompassMDx workstation.

Table 2. Primer Pairs Used to Amplify Single Nucleotide Polymorphisms[a]		
Target	**Forward Primer**	**Reverse Primer**
*CYP2C9*2*	AGT GTC AGC TTC CTC TTT CTT	AGT CCA GTA AGG TCA GTG ATA TG
*CYP2C9*3*	CTA AAG TCC AGG AAG AGA TTG A	GAT ACT ATG AAT TTG GGG ACT TC
VKORC1	TTG GAT TGA TTG AGG ATG CTG TC	ATA GGG TCA GTG ACA TGG AAT C

[a] Forward and reverse polymerase chain reaction primers are shown in the 5′ to 3′ direction for each target. Terminal nucleotides were modified with biotin as previously described.[17]

The imaging software performed all required spot size and location verification, background subtraction, and intensity capture to generate relative intensities of the wild-type and mutant capture probes for each of the 3 alleles. The final readout of results is presented as the combined *2 and *3 genotype of the *CYP2C9* gene, as well as the specific base calling for the *VKORC1* allele.

Thermocycling Conditions

Two separate PCR master mixes were delivered by the robotics of the EncompassMDx workstation to each of the 2 PCR chambers used to analyze each separate sample. One PCR master mix, containing primer pairs designed to amplify the *CYP2C9*2* (430C>T) and *CYP2C9*3* (1075 A>C) loci, along with all required amplification reagents, was introduced into one of the PCR chambers, whereas a second PCR master mix, containing all required reagents to amplify the *VKORC1* (1173 G>A) loci, was introduced into the second PCR reaction chamber (Table 2). In addition, to avoid potential contamination from previously amplified PCR products, all PCR reactions were initially subjected to uracil-*N*-glycosylase (UNG) treatment by activation at 37°C for 10 minutes, followed by inactivation of UNG at 95°C for 2 minutes. Following UNG inactivation, PCR reactions proceeded through a total of 40 cycles, with 10 cycles programmed at 95°C for 30 seconds, 45°C for 30 seconds, and 72°C for 30 seconds; followed by 20 cycles at 95°C for 20 seconds, 45°C for 20 seconds, and 72°C for 20 seconds; followed by 10 additional cycles at 95°C for 15 seconds, 45°C for 15 seconds, and 72°C for 15 seconds.

Table 3. DNA Probes Immobilized on Integrated DNA Array in CARD[a,b]	
Target	**Probe**
*CYP2C9*2*WT	/5AmMC6/ TGAGGA+C+C+GTGTTCA
*CYP2C9*2*MUTA	/5AmMC6/ T+GA+AC+AC+AG+TC+CT+CA
*CYP2C9*2*MUTB	/5AmMC6/ TGAACA+C+A+GTCCTCA
*CYP2C9*3*WT	/5AmMC6/ A+GG+TC+AA+TG+TA+TC+TC
*CYP2C9*3MUT	/5AmMC6/ G+AG A+TA +CCT +TGA +CCT T
*VKORC1*WT	/5AmMC6/ CAT CGA +C+C+C TTG GAC
*VKORC1*MUT	/5AmMC6/ GT+C CA+A GA+G T+CG A+TG A
Spotting control	/5AmMC6/ TTT TTT TTT TTT TTT TTT /3Bio/

[a] Disposable CARD cartridges for the EncompassMDx workstation (Rheonix, Ithaca, New York).

[b] Sequences of capture probes are indicated in the 5′ to 3′ direction. Locked nucleic acid placements are preceded by a plus symbol (+). The capture probe for *CYP2C9*2* contains a mix of *CYP2C9*2*MUTA and B. All probes were aminoterminated on the 5′ end to allow for covalent linkage to the membrane filter via 1-ethyl-3-(3-dimethylaminopropyl)carbodiimide (EDAC) chemistry.[41] The spotting control contains a biotin molecule on 3′ end to allow for direct binding with the streptavidin-coupled horseradish peroxidase.

Detection of Hybridized DNA on Arrays by Reverse Dot Blot

All reverse dot blot incubation steps, except for color development and the final wash, were performed in a solution containing 150 mM NaCl, 10 mM NaH_2PO_4, 1 mM EDTA, and 0.1% sodium dodecyl sulfate. The amplified products generated in each of the 2 separate PCR reaction chambers for each sample or control were diluted with hybridization buffer, heat-denatured by incubation at 98°C for 3 minutes, pooled, and delivered to the DNA arrays for hybridization at 56°C for 10 minutes. Spotted on the arrays were specific probes (Table 3) designed to hybridize to the wild-type or mutant alleles at the 3 different loci. Probes were designed with locked nucleic acids in various positions to increase the differences in melting temperature between exact match and single-base pair mismatched DNA, thus allowing for the distinction of the SNP alleles.[21] Following 2 washes at the hybridization temperature to remove unbound single-stranded DNA, the temperature of the chamber was decreased to 35°C and HRP-conjugated streptavidin was introduced into the chamber and incubated for 5 minutes. After 2 additional washing steps to remove unbound HRP, TMB was introduced and allowed to react at 35°C for 7.5 minutes. The microarray chamber was then washed to remove any unreacted TMB, and the chamber was filled with 20% ethanol in water to capture images without bubbles.

Positive and Negative Controls

Each run of 4 CARDs (ie, 16 samples) contained one positive control and one negative control. The positive control (Maine Molecular Quality Controls, Scarborough, Maine) consisted of synthetic DNA sequences encoding both wild-type and mutant alleles of the *CYP2C9*2*, *CYP2C9*3*, and *VKORC1* SNPs suspended in a proprietary, noninfectious, bloodlike matrix. The controls were processed the same as the authentic blood samples. Because they consisted of both wild-type and mutant alleles of each of the 3 SNPs of interest, a run was deemed valid if all spots were detected on the DNA array. The negative control consisted of a buffer blank applied to the CARD exactly as done with the test samples and was considered to pass if no spots, other than the spotting controls, were detected.

Distinguishing Genotypes

The ability to distinguish the various genotypes was based on the relative intensity of signals at the various locations on the DNA arrays. Briefly, the system's imaging hardware and software were designed to locate each of the 16 "regions of interest" (Figure 1, A and B), corresponding to the mutant and wild-type spots as well as the "spotting controls," and then, to average the signal intensities (based on pixels) within the spots after subtracting the background intensity of 4 loci immediately adjacent to each of the 16 spots (ie, background signals) as noted in Figure 1, C. After completing the analysis for each individual region of interest, corresponding to the various probes, the system's software was programmed to compare the average intensities (beyond background) of the wild-type versus mutant spots and to make genomic "calls" based on the threshold angles determined in this study (see below).

Statistical Methods

The signal intensities were measured on a continuous scale; therefore, to classify samples by genotype, thresholds were derived, based on collected data. For a given patient sample, a pair of signal

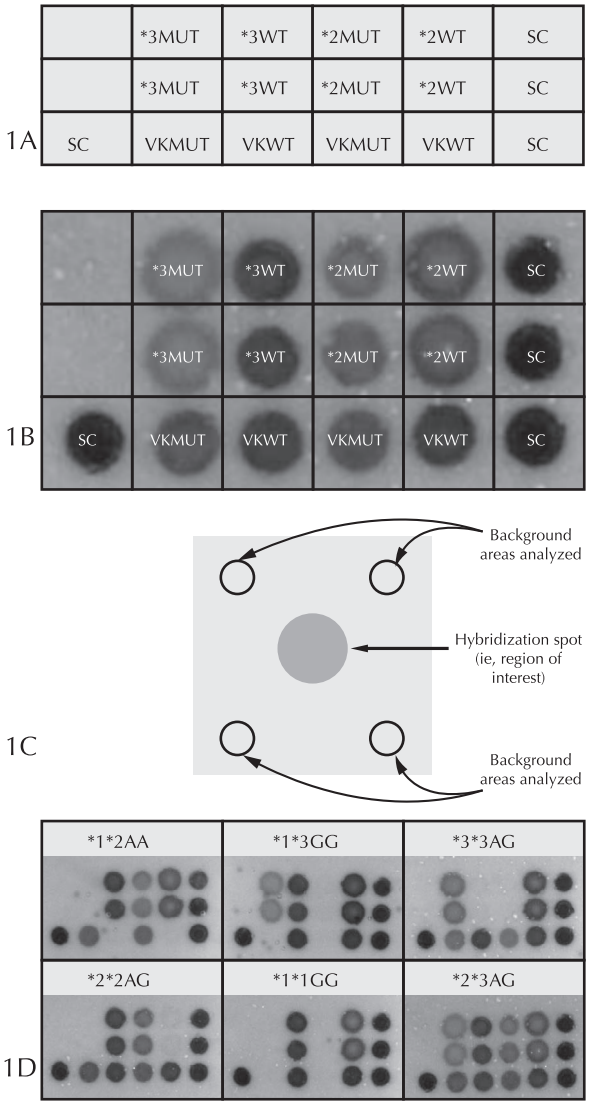

Figure 1. *A, Schematic of DNA array showing the locations of the duplicate probes against the wild-type and mutant alleles for all 3 of the single nucleotide polymorphisms under investigation. In addition, spotting controls (SC), consisting of biotinylated poly(dT),*[17] *are also arrayed, 3 on the right and one on the bottom left. Because each of the SC spots will react with the streptavidinylated horseradish peroxidase, all arrays must display the SC spots in the correct locations, thus confirming the proper orientation of the DNA array within the CARD. B, An image of a filter arising from the analysis of an individual heterozygous for all 3 alleles. The software evaluates the signal intensity within the spots and subtracts the signal intensity of the immediately surrounding area as described in panel C. C, The optic system was designed to determine the intensity of the region of interest after subtracting the intensity of background signals located at 4 adjacent areas. For each allele, the average signal intensity of 2 separate hybridization spots were computed after subtracting the background signals. D, Six representative DNA arrays, demonstrating hybridization spots resulting from multiplex polymerase chain reaction amplification and hybridization to probes immobilized on the array. All possible genotypes for the individual alleles are captured within those 6 arrays (eg, homozygous wild type, heterozygous, and homozygous mutant).* CYP2C9 *genotype descriptions: *1*1, wild type for both *2 and *3 alleles; *1*2, wild type *3 and heterozygous *2; *1*3, wild type *2 and heterozygous *3; *2*3, heterozygous *2 and *3; *2*2, homozygous mutant *2 and wild type *3; *3*3, homozygous mutant *3 and wild type *2.* VKORC1 *genotype descriptions: GG, homozygous wild type; AG, heterozygous; AA, homozygous mutant. In addition to the targets, the 4 SC, in their proper orientation, are shown.*

intensities was obtained, one corresponding to the wild type and one for the mutant, and such data were displayed via a 2-dimensional scatterplot. We hypothesized that genotypes determined by bidirectional DNA sequencing (used as the gold standard) could be differentiated by the automated system according to the standard position of the angle of the sample-specific intensity point. The classification rule assigned those samples that yielded angles less than Θ_1 as *homozygous wild type* and assigned those greater than Θ_2 as *homozygous mutant*. Those samples that fall between Θ_1 and Θ_2 were classified as *heterozygotes*. The diagnostic utility in discriminating genotypes under that working assumption was examined through the generation of the receiver operating characteristic surface, which is a graphic display of the rates of correct genotype classification under all possible angle thresholds. The receiver operating characteristic surface is a generalization of the classic receiver operating characteristic curve in the 3-dimensional case.[22] Pairs of optimal angle thresholds, Θ_1 and Θ_2, for discriminating the 3 possible genotypes for each loci were identified based on the Youden index and the generalized Youden index, under assumed normality, as described by Nakas and Yiannoutsos[23]; the weights required for the generalized Youden index were taken to be the observed prevalence of the genotypes. Once established, the thresholds that permit distinction of the various genotypes were programmed into the system's software for automatic genotype calls. All statistical analyses were performed using SAS software, version 9.3 (SAS Institute, Cary, North Carolina).

Blood Specimens

All blood specimens (n = 254) used in the present study were obtained from the central laboratory of the Catholic Health System (Buffalo, New York) under an institutional review board–approved protocol. All samples were residual specimens provided after all required clinical testing had already been completed. All samples were deidentified with no linkage to the various individuals evaluated.

RESULTS

The automated determination of genotypes derived from blood samples from individuals was accomplished by allowing the fully automated molecular detection system to perform all necessary assay steps unattended. Although the system had previously been shown capable of automatically performing all necessary sample preparations, multiplex PCRs, and detections,[17] it was necessary to "train" the software to discern and report the various possible genotypes at the loci under investigation. Cleary discernible hybridization spots were observed on the DNA arrays after the entire assay was performed automatically (Figure 1, D). In addition to the spots from the amplicon hybridization to the immobilized DNA probes, 3 spotting controls were also clearly visible on the right side of the array, along with one spotting control on the bottom left corner. The visualization and location of those spots not only ensured that the HRP reaction performed correctly but also allowed the imaging software to confirm the proper orientation of the DNA arrays, thereby mitigating the possibility of wrong calls. A "manual" read of the DNA array from the sample shown clearly revealed the hybridization at the wild-type and mutant probes for all 3 loci, resulting in a genotype call of *CYP2C9 *2/*3* and *VKORC1* AG. Because the goal of this study was to evaluate the fully automated process, including the final read out of the results, genotypes established by

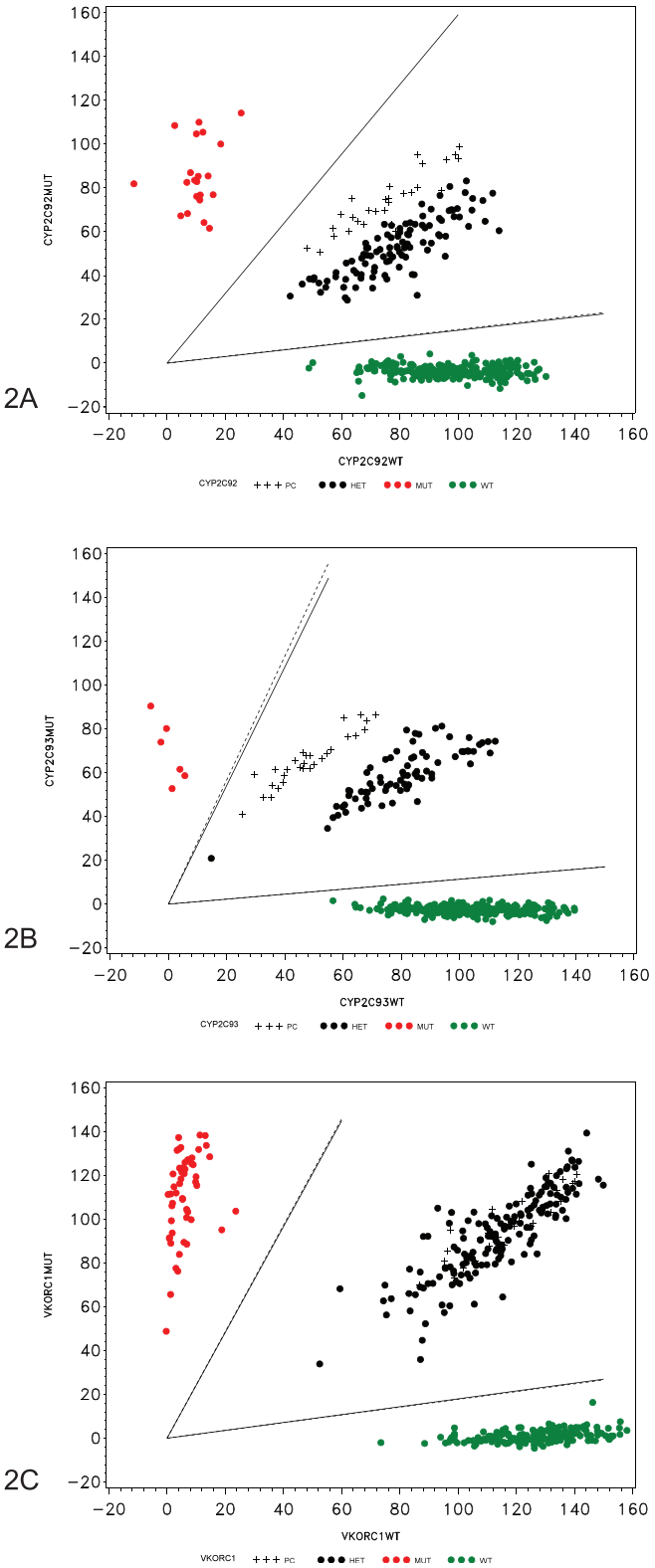

Figure 2. *Scatterplots of sample data corresponding to* CYP2C9*2, CYP2C9*3, *and* VKORC1 *alleles. A, The relative average signal intensities of duplicate hybridization spots for the wild-type* CYP2C9*2 *allele plotted against the relative average signal intensities of duplicate hybridization spots for the mutant allele are shown for all samples and positive controls (PCs) evaluated. The same PC sample (shown as + in the figure), which consists of a cloned plasmid, which was heterozygous for all 3 single nucleotide polymorphisms, was used in all experiments. Because it was heterozygous for all loci, both the wild-type and mutant spots should be detected, resulting in the PCs being located between the* Θ_1 *and* Θ_2 *thresholds. B, The relative average signal intensities of duplicate hybridization spots for the wild-type* CYP2C9*3 *allele plotted against the relative average signal intensities of duplicate hybridization spots for the mutant allele are shown for all samples and PCs evaluated. C, The relative average signal intensities of duplicate hybridization spots for the wild-type* VKORC1 *allele plotted against the relative average signal intensities of duplicate hybridization spots for the mutant allele are shown for all samples and PCs evaluated. The standard position angles used to differentiate the 3 genotypes at each loci were statistically determined using both the Youden index and the adjusted Youden index values to determine* Θ_1 *and* Θ_2*. Using the Youden index method,* Θ_1 *angles were determined to be 8.54, 6.46, and 10.20 for* CYP2C9*2, CYP2C9*3, *and* VKORC1, *respectively. The* Θ_2 *angles were determined to be 57.85, 69.73, and 67.53 for* CYP2C9*2, CYP2C9*3, *and* VKORC1, *respectively. Using the adjusted Youden index method,* Θ_1 *angles were determined to be 8.74, 6.49, and 10.06 for* CYP2C9*2, CYP2C9*3, *and* VKORC1, *respectively. The* Θ_2 *angles were determined to be 58.5, 70.55, and 67.66 for* CYP2C9*2, CYP2C9*3, *and* VKORC1, *respectively.*

bidirectional sequencing were used as the gold standard to program the automated system's software to differentiate among the various possibilities. Although representative, reverse dot blots demonstrated the clarity of results (Figure 1, D), the software was programmed to automatically distinguish the various genotypes. When the relative intensity of the hybridization spots at the wild-type and mutant alleles were compared and plotted against each other (Figure 2, A through C), excellent discrimination among the 3 genotypes at each of the 3 loci was apparent. Ultimately, it was confirmed that the 3 possible genotypes at each loci could be discriminated by the standard position angle thresholds established.

Using the established threshold angles, the genotype calls by the system were compared with the bidirectional DNA sequencing data. A broad representation of genotypes was detected among the samples by bidirectional sequencing (Table 4). At each individual locus, all 3 possible genotypes (ie, homozygous wild type, heterozygous, and homozygous mutant) were detected. In addition, on a combined basis, with the exception of homozygous mutants at both *CYP2C9* loci or either homozygous *CYP2C9* mutation in combination with homozygous mutant at the *VKORC1* loci, all other possible genomic combinations were observed. The system's software reported the same genotypes for each sample as determined by bidirectional sequencing. Moreover, with bidirectional sequencing results serving as the gold standard, no wrong genotype calls were made by the fully automated system.

In addition to the above studies, we independently analyzed 70 samples on each of 3 different EncompassMDx workstations and compared the genotype calls made by the optimized software on each of the 3 separate instruments (Table 5). In all cases, each of the 3 instruments yielded the same genotypes reported by bidirectional DNA sequencing.

Finally, once assured that the software was programmed to correctly call the various genotypes, it was further programmed to print out final reports describing the genotypes of the samples under investigation (Supplemental Figure 2).

COMMENT

The Centers for Medicare and Medicaid, as well as private and commercial payers, have argued that sufficient clinical utility has not been demonstrated for many pharmacoge-

Table 4. Comparison of Bidirectional Sequencing With EncompassMDx Workstation Results[a]

Bidirectional Sequencing Results			EncompassMDx Workstation Results	
CYP2C9	*VKORC1*	Tested, No.	Correct, No.	Agreement, %
*1/*1	GG	82	82	100
*1/*1	GA	62	62	100
*1/*1	AA	25	25	100
*1/*2	GG	20	20	100
*1/*2	GA	22	22	100
*1/*2	AA	4	4	100
*2/*2	GG	5	5	100
*2/*2	GA	3	3	100
*2/*2	AA	0	0	100
*1/*3	GG	10	10	100
*1/*3	GA	7	7	100
*1/*3	AA	2	2	100
*2/*3	GG	2	2	100
*2/*3	GA	4	4	100
*2/*3	AA	3	3	100
*3/*3	GG	1	1	100
*3/*3	GA	2	2	100
*3/*3	AA	0	0	100
Total		**254**	**254**	100

[a] The results obtained with the EncompassMDx workstation (Rheonix, Ithaca, New York) are compared with the bidirectional DNA sequence results as described in the text.

nomics tests. Although not implicitly stated, pharmacoeconomic considerations also have an important role in reimbursement decisions. For example, despite FDA recommendations that prescribing physicians take into consideration the genotypes of patients at the *CYP2C9* and *VKCORC1* loci before initiating anticoagulation therapy, many payers do not routinely reimburse such testing. When compared with an approximately $5.00 reimbursement for prothrombin time and INR testing routinely used to inform warfarin dosing, payers often argue that the high costs associated with many current molecular diagnostic tests are not justified. Taking into consideration the significant costs to the health care system resulting from ADEs associated with improper warfarin dosing,[24] however, the total cost to the system should be considered in reimbursement decisions. According to the Piazza et al[24] study, approximately $40,000 (inclusive of hospitalization and pharmacy costs) can be attributed to each ADE. Warfarin is one of the most widely prescribed drugs in the United States, with more than 30 million prescriptions filled per year,[25] resulting in more than 43 000 ADEs per year.[7,26] Therefore, the total added cost to the health care system from warfarin ADEs is approximately $1.7 billion/y. Factoring in the cost of human suffering and loss of productivity, the routine use of pharmacogenomics testing should be considered. A recent multicenter study[27] in the United States, comparing the clinical utility of genotype-guided versus clinically guided warfarin dosing, indicated no statistically significant improvement in anticoagulation control during the first 4 weeks of therapy, and there were no significant differences in major bleeding or thromboembolisms observed. In contrast, a similar study[28] performed in Europe revealed improved performance with a pharmacogenomics algorithm when evaluated during the first 4 weeks of therapy, although at the study's 12-week endpoint, no differences were observed. Moreover, a third study[29] reported no clinically significant bleeding events in a pharmacogenetic-guided warfarin study group, whereas 3 such events were noted in the control group. Taking those recent studies into consideration, a group from the FDA suggested that, in addition to intermediate endpoints, such as percentage of time in the therapeutic range, uncommon, but clinical meaningful, outcomes, such as ADEs, should also be considered when evaluating the use of pharmacogenetic testing.[30]

Pharmacogenomics testing before the initiation of clopidogrel bisulfate (Plavix, Bristol-Myers Squibb/Sanofi Pharmaceuticals Partnership, Bridgewater, New Jersey) therapy, which must be bioactivated by *CYP2C19* to provide effective antiplatelet protection, has also been recommended by FDA-approved labeling of the drug. Individuals harboring heterozygous mutations at either the *CYP2C19*2* or *CYP2C19*3* loci display significantly reduced bioactivation, and thus, dosing amounts need to be adjusted.[31] Moreover, individuals who are homozygous mutant at either the *CYP2C19*2* or *CYP2C19*3* loci have virtually no ability to convert the drug to its active form, thus prompting the FDA to require a box label indicating that pharmacogenomics data should be considered before initiating drug therapy.[32] Obviously, physicians unaware of the CYP2C19 status of their patients could unknowingly provide no therapeutic benefit to their patients and possibly should have alternative therapies considered. Despite considerable data demonstrating the effect of pharmacogenomics on effective treatment by clopidogrel,[33–37] the reasons often cited for not performing pharmacogenomics testing are the high costs of molecular diagnostic testing, delayed turnaround times, lack of reimbursement, and physicians being unfa-

Table 5. Reproducibility of Results Across 3 Separate EncompassMDx Workstations[a]

Loci	Genotype	Subjects, No.	Genotype "Call"		Agreement, %
			Sequencing (No.)	Instrument (No.)	
*CYP2C9*2*	Homozygous wild type	37	WT (37)	WT (37)	100
	Heterozygous	26	HET (26)	HET (26)	100
	Homozygous mutant	7	MUT (7)	7 (7)	100
*CYP2C9*3*	Homozygous wild type	42	WT (42)	WT (42)	100
	Heterozygous	26	HET (26)	HET (26)	100
	Homozygous mutant	2	MUT (2)	MUT (2)	100
VKORC1	Homozygous wild type	31	WT (31)	WT (31)	100
	Heterozygous	30	HET (30)	HET (30)	100
	Homozygous mutant	9	MUT (9)	MUT (9)	100

Abbreviations: HET, heterozygous, at the specified loci; MUT, homozygous mutant, at the specified loci; WT, homozygous wild type, at the specified loci.

[a] EncompassMDx workstation (Rheonix, Ithaca, New York).

miliar with the underlying molecular biology basis of drug metabolism.[38,39]

To facilitate the use of pharmacogenomic data, we have designed a fully automated molecular detection platform that can dramatically simplify and reduce the cost of the molecular testing. A rapid-ACCE (analytic validity, clinical validity, clinical utility, and ethical, legal, and social implication) review[40] indicates that the cost of performing CYP2C9 and VKORC1 genotyping is $300 to $800 per test, not inclusive of the capital equipment required to perform the assays, which can be $100,000 to $250,000. Because the disposable CARDs are produced by inexpensive, plastic-injection molding methods, significant cost savings can be achieved with an estimated cost to users of $45 per test, inclusive of the equipment costs and all necessary reagents, thus eliminating that obstacle from payers' consideration. Moreover, the system's simplicity will dramatically reduce the training required and decrease the time until results to less than 3 hours. The automated system can also be used to collect large-scale data sets to support clinical utility claims, critically required by payers to support reimbursement. With such reimbursement in place, the automated system should also prove useful in expanding the use of pharmacogenomics data for clinical application, helping to ensure that specific drugs are only administered to those individuals genetically predisposed to obtain the most likely benefit. Not only will cost savings result from providing drugs only to receptive individuals but also additional savings will result from a reduction in hospitalizations from ADEs.

We thank James Jarnot, MBA, MT, of the Catholic Health System (Buffalo, New York) for providing the blood specimens used in this study. In addition, we thank Norma Nowak, PhD (Department of Biochemistry, State University of New York, Buffalo) and Sean Glenn, PhD (Genomics Shared Resource, Roswell Park Cancer Institute, Buffalo) for expert advice and the performance of the Sanger Sequencing, which was supported by Roswell Park Cancer Institute and by grant P30 CA016056 from the National Cancer Institute (Bethesda, Maryland). Financial support from the State University of New York (Buffalo) Center for Advanced Biomedical and Bioengineering Technology partially subsidized the cost of performing the required DNA sequencing.

References

1. Giacomini KM, Yee SW, Ratain MJ, Weinshilboum RM, Kamatani N, Nakamura Y. Pharmacogenomics and patient care: one size does not fit all. *Sci Transl Med*. 2012;4(153):153ps18. doi:10.1126/scitranslmed.3003471.

2. McCarthy JJ, McLeod HL, Ginsburg GS. Genomic medicine: a decade of successes, challenges, and opportunities. *Sci Transl Med*. 2013;5(189):189sr4. doi:10.1126/scitranslmed.3005785.

3. Hresko A, Haga S. Insurance coverage policies for personalized medicine. *J Pers Med*. 2012:2(4):201–216.

4. Sorenson C, Drummond M, Khan BB. Medical Technology as a key driver of rising healthcare expenditure: disengaging the relationship. *Clinicoecon Outcomes Res*. 2013;223–234. doi:10.2147/CEOR.S39634.

5. Bogousslavsky J, Regli F. Anticoagulant-induced intracerebral bleeding in brain ischemia. Evaluation in 200 patients with TIAs, emboli from the heart, and progressing stroke. *Acta Neurol Scand*. 1985;71(6):464–471.

6. Gullov AL, Koefoed BG, Peterson P. Bleeding complications to long-term oral anticoagulant therapy. *J Thromb Thrombolysis*. 1994;1(1):17–25.

7. Landefeld C, Beyth RJ. Anticoagulant-related bleeding: clinical epidemiology, prediction, and prevention. *Am J Med*. 1993;95(3):315–328.

8. Budnitz DS, Lovegrove MC, Shehab N, Richards CL. Emergency hospitalizations for adverse drug events in older Americans. *N Engl J Med*. 2011;365(21):2002–2012.

9. Johnson JA, Gong L, Whirl-Carrillo M, et al; Clinical Pharmacogenetics Implementation Consortium. Clinical pharmacogenetics implementation consortium guidelines for CYP2C9 and VKORC1 genotypes and warfarin dosing. *Clin Pharmacol Ther*. 2011;90(4):625–629.

10. Gage BF, Eby C, Johnson JA, et al. Use of pharmacogenomic and clinical factors to predict the therapeutic doses of warfarin. *Clin Pharmacol Ther*. 2008; 84(3):236–331.

11. Waldelius M, Chen LY, Lindh JD, et al. The largest prospective warfarin-treated cohort supports genetic forecasting. *Blood*. 2009;113(4):784–792.

12. Pavini A, Naushad SM, Rupasree Y, et al. Optimization of warfarin dose by population-specific pharmacogenomic algorithm. *Pharmacogenomics J*. 2012; 12(4):306–311.

13. Kamali F. Genetic influences on the response to warfarin. *Curr Opin Hematol*. 2006;13(5):357–361.

14. Reider MJ, Reiner AP, Gage BF, et al. Effect of VKORC1 haplotypes on transcriptional regulation and warfarin dose. *N Engl J Med*. 2005;352(22):2285–2293.

15. Bristol-Myers Squibb. Coumadin product insert 1205736A4. Princeton, NJ: Bristol-Myers Squibb. http://packageinserts.bms.com/pi/pi_coumadin.pdf. Updated October 2011. Accessed July 8, 2013.

16. Meckley LM, Neuman PJ. Personalized medicine: factors influencing reimbursement. *Health Policy*. 2010;94(2):91–100.

17. Spizz G, Young L, Yasmin R, et al. Rheonix CARD technology: an innovative and fully automated molecular diagnostic device. *Point Care*. 2012; 11(1):42–51.

18. Wallis Y, Morrell N. Automated DNA sequencing. In: Theophilus BDM, Rapley R, eds. *PCR Mutation Detection Protocols*. 2nd ed. New York, NY: Humana Press; 2011:173–185. *Methods in Molecular Biology*; vol 688.

19. Boom R, Sol CJ, Salimans MM, Jansen CL, Wertheim-van Dillen PM, van der Noordaa J. Rapid and simple method for purification of nucleic acids. *J Clin Microbiol*. 1990;28(3):495–503.

20. Zhou P, Young L, Chen Z. Weak solvent based chip lamination and characterization of on-chip valve and pump. *Biomed Microdevices*. 2010;12(5): 821–832.

21. You Y, Moreira BG, Behlke MA, Owczarzy R. Design of LNA probes that improve mismatch discrimination. *Nucl Acids Res*. 2006;34(8):e60 doi:10.1093/nar/gkl175.

22. Nakas CT, Yiannoutsos CT. Ordered multiple-class ROC analysis with continuous measurements. *Stat Med*. 2004;23(22):3437–3449.

23. Nakas CT, Alonzo TA, Yiannoutsos CT. Accuracy and cut-off point selection in three-class classification problems using a generalization of the Youden index. *Stat Med*. 2010;29(28):2946–2955.

24. Piazza G, Nguyen TN, Cios D, et al. Anticoagulation-associated adverse drug events. *Am J Med*. 2011;124(12):1136–1142.

25. Hirsch J, Fuster V, Ansell J, Halperin JL; American Heart Association/American College of Cardiology Foundation. American Heart Association/American College of Cardiology Foundation guide to warfarin therapy. *J Am Coll Cardiol*. 2003;41(9):1633–1652.

26. Douketis JD, Foster GA, Crowther MA, Prins MH, Ginsberg JS. Clinical risk factors and timing of recurrent venous thromboembolism during the initial 3 months of anticoagulant therapy. *Arch Intern Med*. 2000;160(22):3431–3436.

27. Kimmel SE, French B, Kasner SE, et al; COAG Investigators. A pharmacogenetic versus a clinical algorithm for warfarin dosing. *New Eng J Med*. 2013;369(24):2283–2293.

28. Verhoef TI, Ragia G, de Boer A, et al; EU-PACT Group. A randomized trial of genotype-guided dosing of acenocoumarol and phenprocoumon. *New Eng J Med*. 2013;369(24):2304–2312.

29. Pirmohamed M, Burnside G, Eriksson N, et al; EU-PACT Group. A randomized trial of genotype-guided dosing of warfarin. *New Engl J Med*. 2013; 369(24):2294–2303.

30. Zineh I, Pacanowski M, Woodcock J. Pharmacogenetics and coumarin dosing-recalibrating expectations. *New Eng J Med*. 2013;369(24):2273–2275.

31. Mega JL, Close SL, Wiviott SD, et al. Cytochrome P-450 polymorphisms and response to clopidogrel. *New Engl J Med*. 2009;360(4):354–362.

32. Bristol-Myers Squibb. Plavix (clopidogrel bisulfate) product insert. Bridgewater, New Jersey: Bristol-Myers Squibb. http://packageinserts.bms.com/pi/pi_plavix.pdf. Updated December 2013. Accessed December 13, 2013.

33. Gurbel PA, Tantry US. Drug insight: clopidogrel nonresponsiveness. *Nat Clin Pract Cardiovasc Med*. 2006;3(7):387–395.

34. Gurbel PA, Bliden KP, Hiatt BL, O'Connor CM. Clopidogrel for coronary stenting: response variability, drug resistance, and the effect of pretreatment platelet reactivity. *Circulation*. 2003;107(23):2908–2913.

35. Angiolillo DJ, Fernandez-Ortiz A, Bernardo E, et al. Variability in individual responsiveness to clopidogrel: clinical implications, management, and future perspectives. *J Am Coll Cardiol*. 2007;49(14):1505–1516.

36. O'Donoghue M, Wiviott SD. Clopidogrel response variability and future therapies: clopidogrel: does one size fit all? *Circulation*. 2006;114(22):e600–e606. doi:10.1161/CIRCULATIONAHA.106.643171.

37. Shehab N, Sperling LS, Kegler SR, Budnitz D/s. National estimates of emergency department visits for hemorrhage-related adverse events from clopidogrel plus aspirin and from warfarin. *Arch Intern Med*. 2010;170(21): 1926–1933.

38. Perry CG, Shuldiner AR. Pharmacogenomics of anti-platelet therapy: how much evidence is enough for clinical implementation? *J Hum Genet*. 2013;58(6): 339–345.

39. Manolio TA, Chisholm RL, Ozenberger B, et al. Implementing genomic medicine in the clinic: the future is here. *Genet Med*. 2013;15(4):258–267.

40. McClain MR, Palomaki GE, Piper M, Haddow JE. A rapid-ACCE review of *CYP2C9* and *VKORC1* alleles to inform warfarin dosing in adults at elevated risk for thrombotic events to avoid serious bleeding. *Genet Med*. 2008;10(2): 89–98.

41. Zhang Y, Coyne MY, Will SG, Levenson CH, Kawasaki ES. Single-base mutational analysis of cancer and genetic diseases using membrane bound modified oligonucleotides. *Nucleic Acids Res*. 1991;19(14):3929–3933.